PAPER

Check for updates

Interplay of the structures and viscoelastic properties of polyampholyte gels with the interlude of neutral blocks

You Cai Xue,†[ab] Yi Hui Zhao,†[ab] Xiu Li Sun[c] and Di Jia 🆔 *[ab]

Polyampholyte gels with hierarchical structures due to the microphase separation are good candidates for biomaterials and bioengineering due to their unique properties such as self-healing and anti-biofouling. However, how to precisely control their microstructures and viscoelastic properties is yet to be explored. By introducing the acrylamide neutral blocks, we have quantitively tuned the micro-structures and viscoelastic properties of polyampholyte gels. With the interlude of more acrylamide neutral blocks, the size and density of the ionic clusters become smaller, leading to a shorter relaxation time. Very small angle neutron scattering results show that the interlude of hydrophilic acrylamide neutral blocks will act as defects to suppress the phase separation and make the microphase separated domains become smaller. In the yielding measurements, the reversible dissociation–association dynamical behavior of the ionic bonds can protect the gels from yielding, exhibiting excellent self-healing properties. The interlude of acrylamide neutral blocks would act as defects to disrupt the formation of ionic bonds, thus making the yielding point decrease. Finally, the impact of different swelling methods on the viscoelastic properties was also studied. Only for gels with intermediate ionic bond strength, can the association–dissociation collective dynamical behavior of the ionic bonds be observed, so they can exhibit excellent self-healing properties. When the ionic bond strength is too strong or too weak, the self-healing properties would disappear. Our work enables us to mimic biological tissues such as mucus, vitreous humor, and nucleus pulposus with desirable viscoelastic properties and self-healing behaviors.

Introduction

Contrasting the irreversible permanent structures created by covalent bonds in chemical gels, physical gels with non-covalent bonds have amazing attributes such as self-healing, time-programmable, recycling, and adhesive properties. Double-network hydrogels composed of one network formed by covalent bonds and the other network formed by non-covalent bonds such as reversible dynamic bonds have been developed to enhance the mechanical performance,[1–6] allowing them to adapt to a broad field of applications such as wound dressings, tissue engineering, *etc.* During the deformation, the reversible dynamic bonds can dissipate energy as a sacrificial network through breaking, thereby enhancing the mechanical properties of the double-network hydrogels.[7,8] For example,

Zhang *et al.* have significantly enhanced the mechanical properties of hydrogels by introducing charged poly(sodium acrylate) into poly(vinyl alcohol) (PVA) hydrogels. The polyelectrolyte-induced aggregation and crystallization of PVA lead to the formation of additional crystalline regions within the hydrogel network. These crystalline regions act as effective cross-linking points, and the formation of double-network hydrogels has significantly improved the mechanical performance and can be used as a biomedical patch.[9] In another example, by adding glucose and tannic acid in the polyacrylamide hydrogels to form a double-network through hydrogen bonds, the hydrogels would be swelling-resistant with strong toughness, good self-recoverability, rapid self-healing and adhesiveness.[10,11] Mu and colleagues prepared polyacrylamide-*co*-acrylic acid/sodium alginate/tannic acid hydrogels through the soaking method. Due to the synergistic effect of hydrogen bonds and covalent bonds within the hydrogels, they can exhibit excellent mechanical properties and adhesive strength, providing new possibilities for the application of hydrogels in a wet environment.[12]

Polyampholyte gels, which consist of anionic monomers and cationic monomers randomly distributed within the polymer

a State Key Laboratory of Polymer Physics and Chemistry, Beijing National Laboratory for Molecular Sciences, Institute of Chemistry, Chinese Academy of Sciences, Beijing 100190, China. E-mail: jiadi11@iccas.ac.cn

b University of Chinese Academy of Sciences, Beijing 100049, China

c Department of Obstetrics and Gynecology, Peking University People's Hospital, Beijing, 100044, China

† Y. C. X. and Y. H. Z. contributed equally to this work.

gel network, have rich viscoelastic properties and fatigue resistance, and they also exhibit excellent biological underwater adhesive properties and anti-biofouling properties, thus making them good candidates as biomaterials.[13–16] Li *et al.* investigated the physical mechanisms of the fatigue resistance of a polyampholyte hydrogel which is composed of hierarchical structures including ionic bonds, transient and permanent polymer networks, and a bicontinuous microphase separated network. It was found that ionic bonds endow the hydrogel with self-healing capabilities, while the bicontinuous microphase separated networks play a dominant role in the long-term memory effects and fracture resistance under cyclic stretching.[17] Gong and colleagues studied the effect of the mesoscale structures of polyampholyte gels on fatigue-delaying behavior and found that the mesoscale structures play a vital role in fatigue resistance of the gels and control the mechanisms of crack propagation.[18–22] For example, the bicontinuous phase networks can significantly decelerate the crack advance until the rupture of the hard phase network. Besides, in the polyampholyte gels there are two kinds of ionic bonds: strong ionic bonds and weak ionic bonds, and the strong ionic bonds serve as permanent crosslinks to maintain the shape of the gel, whereas the weak ionic bonds perform as sacrificial bonds to enhance the fracture resistance by bond rupture and therefore toughen the materials.[13,23] Gong's team also discovered that the shrinking and swelling kinetics of polyampholyte hydrogels is asymmetric. Specifically, the swelling kinetics is governed by the permanently crosslinked network structure, whereas the shrinking kinetics is governed by structure frustration, formed due to large differences in the heat and solvent diffusions. Such an asymmetric swelling/shrinking kinetics is designed to mimic the brainlike memorizing–forgetting behavior.[24,25] Moreover, Baker *et al.* studied the swelling properties of polyampholyte gels with neutral monomer acrylamide and they found that hydrogel swelling increases as the NaCl salt concentration increases, exhibiting an antipolyelectrolyte behavior.[26] Peiffer and Lundberg investigated the viscometric properties of low charge density ampholytic ionomers and found that the separation of these oppositely charged monomer units *via* neutral acrylamide moieties establishes a control over the physical properties not readily attainable in the highly charged polyampholytes.[27] However, how to precisely control and design the desired viscoelastic properties of the polyampholyte gels is yet to be explored.

In this work, by introducing neutral acrylamide blocks containing hydrogen bonds in a polyampholyte gel containing ionic bonds, we explored how to precisely control and design the desired viscoelastic properties of the weakly chemical-crosslinked (0.5%) gels containing both hydrogen bonds and ionic bonds. By employing the very small angle neutron scattering (VSANS) measurements for gels with different fractions of acrylamide neutral blocks and also different monomer concentrations, we have systematically studied the interplay between the microscopic phase-separated structures and the macroscopic viscoelastic properties of the gels containing both hydrogen bonds and ionic bonds. Finally, the impact of different

swelling methods on the viscoelastic properties was investigated. This work helps us better understand the interplay between the microstructures and the viscoelastic properties of polyampholyte gels with the interlude of neutral blocks. It can also enable us to mimic biological tissues such as mucus, vitreous humor, and nucleus pulposus with desirable viscoelastic properties and self-healing behaviors.

Experimental section

Materials

Anionic monomer sodium *p*-styrene sulfonate (NaSS, ≥90%, Sigma-Aldrich), cationic monomer 3-(methacryloylamino)propyl-trimethylammonium chloride (MPTC, 50 wt% in water, Sigma-Aldrich), neutral monomer acrylamide (AM, 40 wt% in water, Sigma-Aldrich), chemical crosslinker N,N′-methylenebis(acrylamide) (MBAA, 2 wt% in water, Macklin), UV initiator α-ketoglutaric acid (99%, Sigma-Aldrich), sodium chloride (NaCl, 99.8%, Macklin), calcium chloride anhydrous (CaCl$_2$, 94%, Macklin), and barium chloride (BaCl$_2$, 99%, Macklin) were used as received. Deionized water was obtained from a Milli-Q water purification system (Millipore, Bedford, MA, USA).

Synthesis of polyampholyte hydrogels

Polyampholyte hydrogels were synthesized using the one-step free-radical copolymerization of the anionic monomer sodium *p*-styrene sulfonate (NaSS), the cationic monomer 3-(methacryloylamino)propyl-trimethylammonium chloride (MPTC), and the neutral monomer acrylamide (AM).[22,23] The chemical crosslinking density is 0.5% with the addition of N,N′-methylenebis(acrylamide) (MBAA) chemical crosslinkers. The chemical crosslinking density of a gel is defined as the molar ratio of the chemical crosslinkers to the total moles of all the monomers and chemical crosslinkers. In all the experiments, there are three tunable parameters, which are the total monomer concentration C_m of anionic monomer NaSS, cationic monomer MPTC and neutral monomer AM (C_m = [NaSS] + [MPTC] + [AM]), the fraction of neutral monomer f = [AM]/C_m, and the salt concentration C_s. The molar charge ratio of the anionic monomer to the total charged monomers r = [NaSS]/([NaSS] + [MPTC]) was fixed at the charge balance point r = 0.52 for all the experiments.[13] The synthetic procedure for the gels with C_m = 1.5 M and f = 30% in the as-prepared state is described below as a typical example. 3.41 g of NaSS, 6.606 mL 50% (w/v) of MPTC solution, 2.399 mL 40% (w/v) of AM solution, 1.734 mL 2% (w/v) of MBAA solution and 32.9 mg of UV initiator α-ketoglutaric acid were mixed with deionized water to bring a total volume of 30 mL. The pre-gel solution was stirred to make it homogenous and transferred to a Petri dish and was sealed. Then, the pre-gel solution was bubbled with nitrogen for 30 min to remove any dissolved oxygen. The reaction is initiated by UV light radiation with a wavelength of 365 nm, and the reaction was continued for 10 hours at room temperature. After polymerization, the as-prepared gel was obtained, and ^{1}H-NMR results show that the

chemical conversion of all the monomers is nearly 100% (for details, see Fig. S1).

Very small angle neutron scattering (VSANS)

VSANS experiments were performed by using the very small angle neutron scattering (VSANS) instrument BL-14[28,29] at the China Spallation Neutron Source (CSNS). Neutron data were collected with a wavelength range from 2.2 Å to 6.7 Å, employing a collimation length of 12.75 m. Samples were encased in quartz cells with an optical path length of 1 mm. Data reduction was performed using the direct beam method, including the measurement of the direct beam,[28,29] solid angle and transmission correction as well as solvent scattering background (or quartz empty cell scattering background) subtraction. VSANS patterns were continuously recorded with an acquisition time of 7200 s. The 1D profiles were fitted with models by using SasView software. The samples for VSANS measurements were synthesized by using deuterated water as the solvent.

Rheological measurements

Rheological measurements were performed on a stress-controlled rheometer (Anton Paar MCR 502) with a 25 mm roughened parallel-plate geometry. Dynamic strain sweep measurements were conducted first to determine the linear viscoelastic region,[30–32] then the dynamic frequency sweep measurements were conducted in the linear viscoelastic region with shear strain fixed at $\gamma = 1\%$. Dynamic strain sweep measurements were conducted at a fixed frequency $\omega = 1$ rad s^{-1}, depending on the samples. All the measurements were carried out at room temperature. Silicon oil was coated on the edge of the parallel plate to prevent water evaporation. The results are reproducible with this protocol, and all the rheological measurements were conducted three times for three gel samples to ensure that the results are reproducible.

Results and discussion

By introducing the acrylamide neutral blocks, the hierarchical structures and viscoelastic properties of the polyampholyte gels were investigated. We systematically changed the compositions of the gels, including the total monomer concentration C_m, the fraction of acrylamide neutral monomers f, and the ionic strength C_s within the gels. In all the experiments, the chemical crosslinking density was fixed at 0.5%, thus they are weakly chemically crosslinked. And the molar charge ratio of anionic monomers to the total charged monomers was fixed at a stoichiometric charge ratio of $r = 0.52$.[13]

The very small angle neutron scattering (VSANS) technique is used to explore the microstructure of the polyampholyte gels. The VSANS profiles of the polyampholyte gels with different fractions of acrylamide neutral blocks f at the fixed monomer concentration $C_m = 1.5$ M were investigated. Deuterated water was used as the solvent for all the VSANS measurements. A Lorentzian peak model was used to fit the VSANS profiles as

follows:[33]

$$I(q) = \frac{\text{scale}}{\left(1 + \left(\frac{q - q_0}{B}\right)^2\right)} + \text{background} \qquad (1)$$

where q_0 is the peak position and B is the full width at half-maximum. The angular conversion between scattering vector q_0 and the correlation length ξ is $q_0 = 2\pi/\xi$. Polyampholyte gels have microphase separated structures composed of a polymer-dense phase and a polymer-poor phase.[18,19,23] Here, the correlation length ξ is identified as the spacing between adjacent two microphase separated domains. From the fitting results, we can get the correlation length $\xi = 654$ nm for $f = 0\%$, $\xi = 265$ nm for $f = 20\%$ (Fig. 1(a) and (b)), $\xi = 239$ nm for $f = 30\%$ and $\xi = 214$ nm for $f = 50\%$ (Fig. S2a and b), respectively. Besides, when $f = 80\%$ and $f = 100\%$, there is almost no phase separated structure and the signals from VSANS measurements are too low to fit the data (Fig. S2c and d). Based on Gong's and others' studies, the phase-separated structures of polyampholyte gels are driven by the Coulombic interaction of the ionic bonds and hydrophobic interactions, and the decrease of hydrophobicity of the monomers or the increase of the chemical crosslinking density can suppress the phase separation in the polyampholyte gels.[19,23] For the weakly chemical crosslinked polyampholyte gels studied here, as f increases, the interlude of hydrophilic acrylamide neutral blocks will act as defects to suppress the phase separation and make the microphase separated domains become smaller. Therefore, the microphase separated structures become smaller with smaller correlation length ξ as f increases from 0 to 50% (Fig. 1(e)). Moreover, the gels with different monomer concentrations C_m at the fixed $f = 20\%$ were also investigated. The VSANS data fitting shows that as C_m increases from 1.0 M to 2.0 M, the correlation length ξ decreases from 496 nm to 166 nm (Fig. 1(b)–(f)). When the monomer concentration C_m increases, the gels will have more topological entanglements, which act as permanent effective cross-linkers to suppress the phase separation, leading to smaller microphase separated domains, as schematically illustrated in Fig. 1(g) and (h). Moreover, polyampholyte gels exhibit hierarchical structures at different length scales.[18,19,23] The polymer-dense microphase separated domains consist of ionic clusters at smaller length scales (Fig. 1(g) and (h)), and these ionic clusters are composed of reversible ionic bonds.

The impact of the fraction of acrylamide neutral blocks f on the viscoelastic properties of the gels was investigated. All the gels studied were weakly chemically crosslinked (0.5% chemical crosslinking density) in the as-prepared state with the same $C_m = 1.5$ M and different f. The gels without acrylamide neutral blocks ($f = 0$) were also studied as the control. Fig. 2(a) is the dynamical frequency sweeps of the gels with different f in the linear viscoelastic region. Fig. 2(b) is the summary of f dependence of the elastic modulus G' obtained from the dynamic frequency sweeps at $\omega = 10$ rad s^{-1} and the crossover points ω_c of elastic modulus G' and loss modulus G''. As shown in Fig. 2(b), the elastic modulus G' decreases from 13.6 kPa to 6.2 kPa as f increases from 0 to 100%. As f increases,
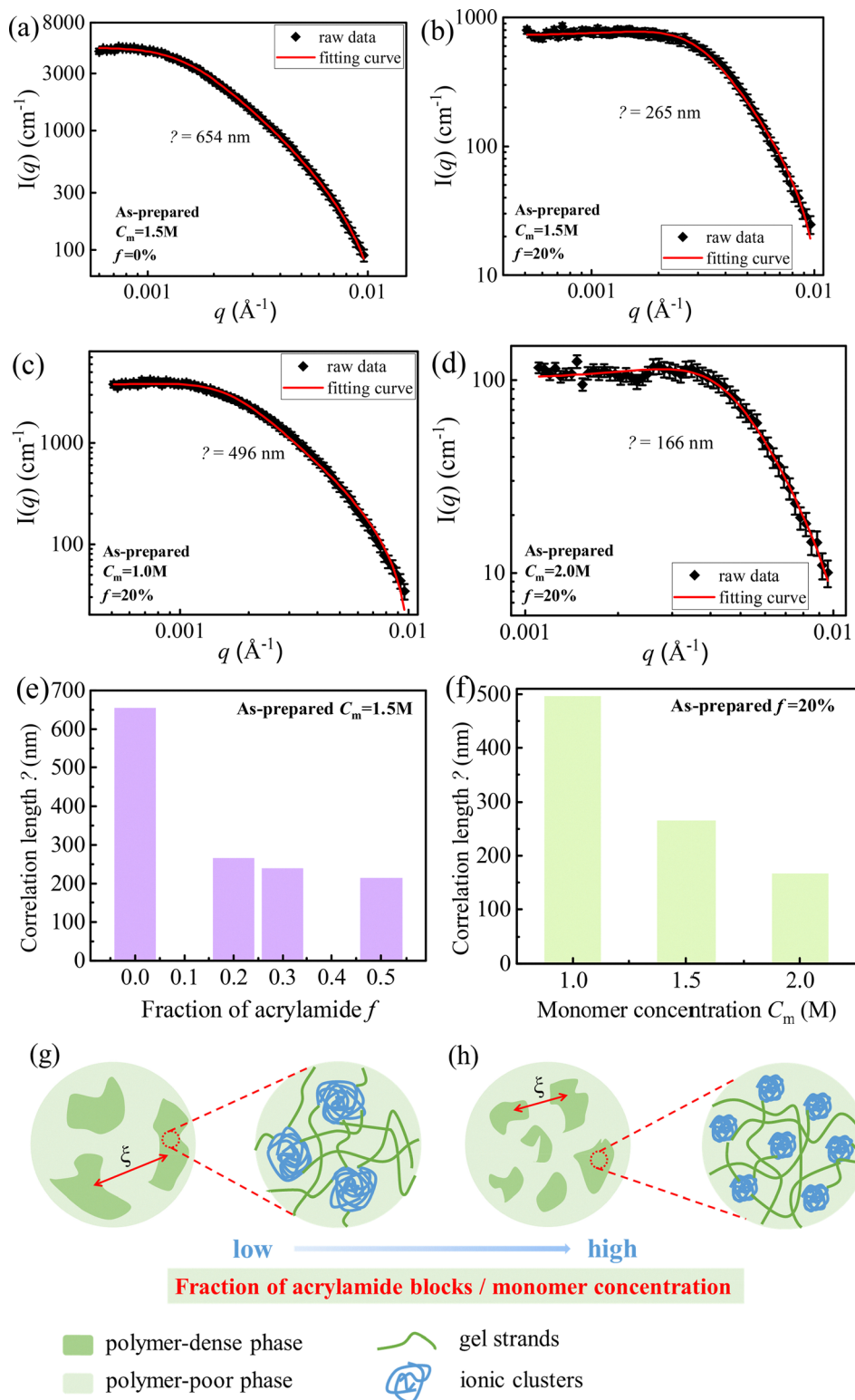
Fig. 1 (a) and (b) Very small angle neutron scattering (VSANS) profiles of the polyampholyte gels with the fraction of acrylamide neutral blocks $f = 0$ (a) and $f = 20\%$ (b) at the same monomer concentration $C_m = 1.5$ M. Raw data (black squares) are fitted with the Lorentzian peak model, and from the fitting curve (red line) the correlation length ξ can be obtained. (c) and (d) Very small angle neutron scattering (VSANS) profiles of the polyampholyte gels with $f = 20\%$ at the monomer concentration $C_m = 1.0$ M (c) and $C_m = 2.0$ M (d). Raw data (black squares) are fitted with the Lorentzian peak model, and from the fitting curve (red line) the correlation length ξ can be obtained. (e) Summary of the correlation length ξ for the polyampholyte gels with different fractions of acrylamide neutral blocks f at fixed monomer concentration $C_m = 1.5$ M. (f) Summary of the correlation length ξ for the polyampholyte gels with different monomer concentrations C_m at fixed $f = 20\%$. (g) and (h) Schematic illustration of the hierarchical polyampholyte gel structures with increasing f or increasing C_m.
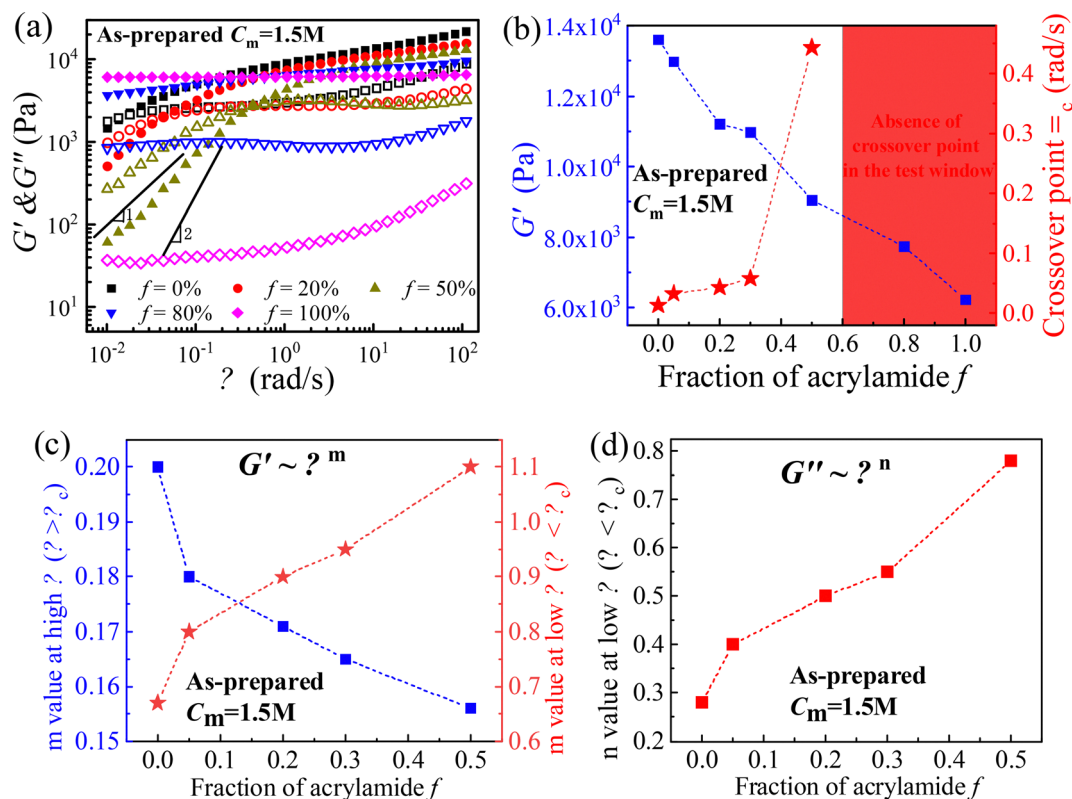
Fig. 2 (a) Dynamic frequency sweeps of the as-prepared gels with the fixed total monomer concentration C_m = 1.5 M, 0.5% chemical crosslinking density, and with different fractions of acrylamide f. The shear strain is fixed at γ = 1%. Closed (open) symbols represent storage (loss) modulus. (b) A summary of elastic modulus G' obtained from dynamic frequency sweeps at ω = 10 rad s^{-1} and the crossover points ω_c of G' & G'' for the as-prepared gels with C_m = 1.5 M and different f. (c) f dependence of m values in the high ($\omega > \omega_c$) and low frequency regions ($\omega < \omega_c$), respectively, for the as-prepared gels with C_m = 1.5 M and $f \leq 50\%$ ($G' \sim \omega^m$, $G'' \sim \omega^n$). (d) Fraction of acrylamide f dependence of n values in the low frequency region ($\omega < \omega_c$) for as-prepared gels with C_m = 1.5 M and $f \leq 50\%$.

the interlude of acrylamide neutral blocks acts as defects to prevent the formation of ion bond pairs between cationic monomers and anionic monomers. Thus, the number of ionic bonds decreases with increasing f. All the gels are weakly chemically crosslinked with the same chemical crosslinking density (0.5%) and the same total monomer concentration (C_m = 1.5 M), so that all the gels have the same number of chemical bonds. Therefore, the decrease of G' with f is due to the decrease of the number of physically ionic bonds. Moreover, as shown from the VSANS data in Fig. 1, as the fraction of acrylamide f increases, the interlude of hydrophilic acrylamide neutral blocks will act as defects to suppress the phase separation and make the microphase separated domains become smaller with smaller correlation length ξ. This will also lead to the decrease of the elastic modulus G'.

Besides, the crossover point ω_c of G' and G'' shifts towards higher frequency as f increases from 0 to 50%, and ω_c disappears when f is above 50% (Fig. 2(a) and (b)). Specifically, ω_c = 0.0136 rad s^{-1}, 0.044 rad s^{-1} and 0.443 rad s^{-1} for f = 0, 20% and 50%, respectively. At high frequencies, they exhibit solid-like characteristics with $G' > G''$, indicating that their response is elastically dominated. While at low frequencies, their behavior is similar to a weak gel, implying viscoelastic liquid-like properties with $G' < G''$, suggesting that their response is

predominantly viscous.[34] Based on the hierarchical structures of the polyampholyte gels composed of ionic bonds,[17,22,23] the crossover points may arise from the collective dynamical behavior of association–dissociation of the ionic clusters and the full relaxation of the topological entanglements. Thus, after the full relaxation they exhibit viscoelastic liquid-like behavior. With the interlude of more neutral acrylamide monomers (larger f), the size and density of the ionic clusters become smaller, leading to a higher crossover point ω_c and a shorter characteristic relaxation time to make the dynamical ionic clusters and topological entanglements fully relax. When f is above 50%, the crossover point ω_c disappears (Fig. 2(a) and (b)). For pure polyacrylamide gel with f = 100%, it is a typical chemical gel with G' being independent of frequency ω, and G' is two orders of magnitude higher than the loss modulus G'', indicating the elastic nature of the polyacrylamide gel (Fig. 2(a)). Therefore, as f increases the gel networks gradually transfer from physical gels to chemical gels. Moreover, the physical bonds play a vital role in the terminal relaxation behaviors when the gels are weakly chemically crosslinked (Fig. S3).[35] However, when the chemical crosslinking density is high, then it will go back to the normal chemical gel behavior that the terminal relaxation would be dominated by chemical crosslinks.

Typically, for chemically crosslinked gels, the storage modulus G' has no frequency dependence, and G' is an order of magnitude higher than the loss modulus G'', indicating the elastic nature of the gels.[36,37] While for physical gels composed of ionic bonds, they can be well described by the sticky Rouse motion of associating polymer strands derived from the ionic bonds (stickers) with $G' \sim \omega^m$, $G'' \sim \omega^n$ ($n = m = 0.5$).[22,38] When f is in the range of 0–50%, both G' and G'' have a strong frequency dependence (Fig. 2(a)), indicating they are more like physical gels with ionic bonds, though they are weakly chemically crosslinked. And they exhibit different frequency dependence in the high frequency ($\omega > \omega_c$) and low frequency ($\omega < \omega_c$) regions (Fig. 2(c) and (d)). In the high frequency region ($\omega > \omega_c$), G' shows weaker frequency dependence and m decreases from 0.2 to 0.15 as f increases from 0 to 50% (Fig. 2(c)). Here, m values deviate from the sticky Rouse relaxation of ionic associations ($m = 0.5$), probably due to the distribution in the strength of the ionic bonds, which is consistent with the previous results.[21,22,39,40] While in the low frequency region ($\omega < \omega_c$), they exhibit viscoelastic liquid-like behavior ($G' < G''$)

with $m > 0.5$ and $n < m$; both m and n values increase with f (Fig. 2(c) and (d)).

The impact of the fraction of acrylamide neutral blocks f on the yielding behaviors in the nonlinear viscoelastic region was also studied. All the gels studied were weakly chemically crosslinked (0.5% chemical crosslinking density) in the as-prepared state with the same $C_m = 1.5$ M and different f. The shear strain sweeps at fixed frequency $\omega = 1$ rad s^{-1} are shown in Fig. 3(a) and (b). For gels with $f \leq 50\%$, both G' and G'' are nearly constant in the linear viscoelastic regime at low shear strain γ before yielding (Fig. 3(a)). As the shear strain γ further increases, G' and G'' start to decrease, leading to the yielding and destruction of the gel structures. For gels with $f = 80\%$ and 100%, although G' is nearly constant in the linear viscoelastic regime before yielding, G'' first increases and then decreases to form a peak, and the peak position, where G'' reaches the maximum, coincides with the yielding point γ_c (Fig. 3(b)), indicating large energy dissipation needed for the yielding and destruction of the gel structures.[32] This is because for polyacrylamide gels, there are hydrogen bonds between amide
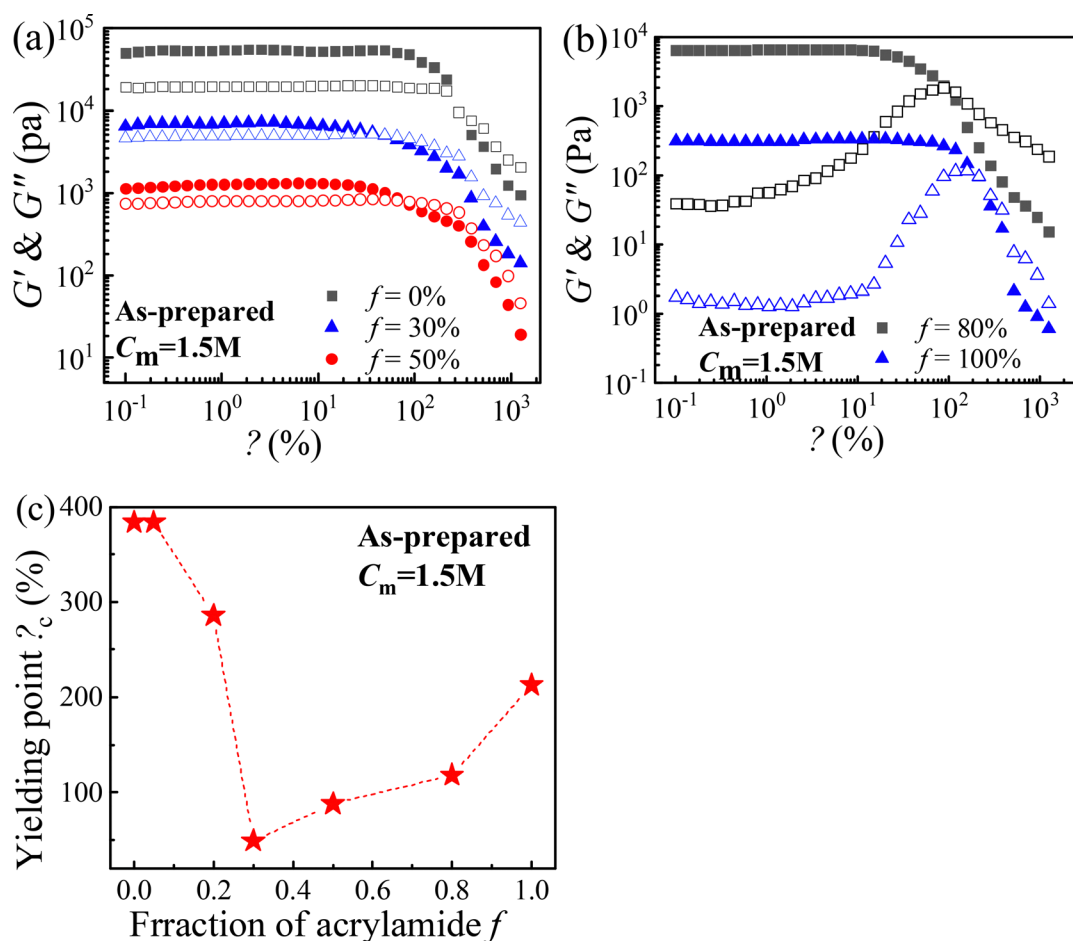
Fig. 3 (a) and (b) Shear strain sweeps at $\omega = 1$ rad s^{-1} for the as-prepared gels with fixed total monomer concentration $C_m = 1.5$ mol L^{-1} and different f, (a) $f = 0\%$, 30% and 50%; (b) $f = 80\%$ and 100%. Closed (open) symbols represent storage (loss) modulus. For a clear vision, the data of $f = 0\%$ and $f = 50\%$ in (a) are shifted by 6× and 6/, respectively. The data of $f = 100\%$ in (b) are shifted by 20/. (c) A summary of the yielding points obtained from shear strain sweeps for gels in the as-prepared state with $C_m = 1.5$ mol L^{-1} and different f.

groups. As documented in the literature, the bond binding energy of hydrogen bonds between amide groups is almost two times higher than that of the ionic bonds between sulfonate groups and ammonium groups.[41,42] Therefore, the breakage of hydrogen bonds in the gels needs to dissipate more energy compared to the breakage of ionic bonds, thus the loss modulus G'' would exhibit a peak for gels with $f = 80\%$ and 100%.

On the other hand, the bond binding energy of hydrogen bonds is higher than that of the ionic bonds, thus hydrogen bonds are more like "permanent bonds", while the ionic bonds are reversible and can offer excellent self-healing properties for the gels. For pure polyampholyte gels ($f = 0\%$), the yielding point γ_c is 384% (Fig. 3(a)) due to the excellent self-healing properties arising from the reversible dissociation–association of the ionic bonds. Here, the yielding point γ_c is defined as the crossover point of G' and G''. As the shear strain γ increases, some relatively weaker ionic bonds would break up first and the rest of the associated ionic bonds and the chemical bonds would support and protect the gel network from yielding. Meanwhile, the previously broken ionic bonds can self-heal and reform again and continue to support the gel network. Such self-healing ionic bonds in turn might also protect and delay the breakage of the chemical bonds at relatively larger shear strain. Therefore, the association–dissociation dynamical process of the self-healing ionic bonds can support the gel network and prevent yielding until under very large shear strain.

As the fraction of acrylamide neutral blocks f increases from 0 to 30%, the yielding point γ_c decreases significantly from 384% to 48.8% (Fig. 3(c)). When the ionic bonds dominate at small f, the association–dissociation of self-healing ionic bonds would make the gels yield at very large shear strain γ_c. Meanwhile the interlude of acrylamide neutral blocks would act as defects to disrupt the formation of ionic bonds. Especially, the yielding point reaches the minimum ($\gamma_c = 48.8\%$) at $f = 30\%$ (Fig. 3(c)). Because when f is 30%, there are roughly one-third neutral monomers, one-third anionic monomers, and one-third cationic monomers in the gel network. Therefore, on

average there is always a defect neutral monomer sitting in between a cationic monomer and an anionic monomer to prevent the formation of ionic bond pairs, so that the number of both the self-healing ionic bonds and the hydrogen bonds reaches the minimum, thus leading to the smallest yielding point γ_c. As f further increases, the yielding point γ_c slightly increases until $\gamma_c = 213\%$ for pure polyacrylamide gels ($f = 100\%$). Because when hydrogen bonds dominate at large f, in addition to the chemical bonds, hydrogen bonds would also provide extra support to protect the gels during deformation. However, the yielding point of pure polyacrylamide gels ($f = 100\%$) is still much lower than that of pure polyampholyte gels ($f = 0$) due to the excellent self-healing properties arising from the reversible dissociation–association of the ionic bonds. Besides, the yielding points γ_c is independent of frequency (Fig. S4 and Table S1), indicating that the transient structures of the gels do not change in the frequency range studied here.

The total monomer concentration C_m dependence was also studied for gels with fixed chemical crosslinking density (0.5%) and $f = 20\%$. As shown in Fig. 4(a), the elastic modulus G' increases with the total monomer concentration C_m. As C_m increases, the gels will have more topological entanglements, which can act as permanent effective cross-linkers to suppress the phase separation with smaller correlation length ξ, as shown in the VSANS data (Fig. 1(f)). However, these topological entanglements act as permanently effective cross-linkers to make the elastic modulus G' increase. As the total monomer concentration C_m increases, G' increases by following $G' \sim C_m^{2.3}$ (Fig. 4(b)), which is consistent with the results of previous studies for polyampholyte gels.[18,19,43] Since the topological entanglement concentration (C_e) between polymer chains follows the scaling law of $C_e \sim C_m^{2.3}$, and here the gels are weakly chemically crosslinked with 0.5% chemical cross-linking density, the topological entanglement is a dominant factor contributing to the moduli of the gel network, thus they follow the scaling law of $G' \sim C_m^{2.3}$.

Besides, both G' and G'' show less frequency dependence with increasing C_m (Fig. 4(a)). As C_m increases from 0.8 M to
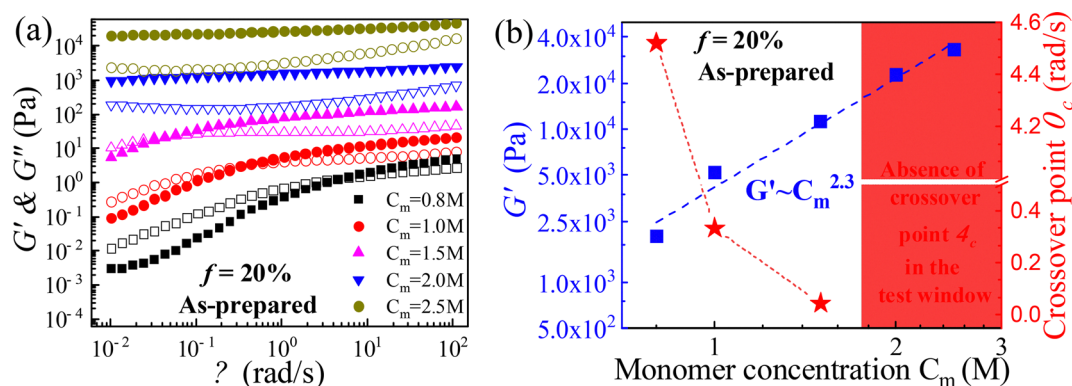
Fig. 4 (a) Dynamic frequency sweeps of the polyampholyte gels in the as-prepared state with $f = 20\%$ and different total monomer concentrations C_m. The shear strain is fixed at $\gamma = 1\%$. Closed (open) symbols represent storage (loss) moduli. For a clear vision, the data in (a) are shifted by 12/, 95/, 420/, and 1000/ for C_m = 2.0 M, 1.5 M, 1.0 M, and 0.8 M, respectively. (b) Elastic modulus G' obtained from dynamic frequency sweeps at $\omega = 10$ rad s^{-1} and the crossover points ω_c of G' & G'' for the as-prepared gels as a plot of C_m for $f = 20\%$.

1.5 M, the crossover points ω_c decrease two orders of magnitude from 4.52 rad s^{-1} to 0.0435 rad s^{-1}. The crossover points ω_c may arise from the dynamical association–dissociation of the ionic clusters and the full relaxation of the topological entanglements. As C_m increases, the number of topological entanglements and ionic bonds increases, thus the gel networks need a longer relaxation time to fully relax and ω_c shifts towards lower frequency (Fig. 4(b)). As C_m further increases to 2.0 M and 2.5 M, the number of topological entanglements and ionic bonds is so high that their characteristic relaxation time is too long and is out of the experimental observation time scale here. Besides, they become chemical gels since G' is independent of frequency and is one order of magnitude higher than G'', indicating their elastic nature, and G'' exhibits a minimum. Therefore, as C_m increases the gels transfer from physical gels to more like chemical gels. We also investigated C_m dependence for gels with f = 50% and 0.5% chemical crosslinking density. They exhibit similar trends to those of gels with f = 20% (see Fig. S5).

Finally, the impact of different swelling methods on the viscoelastic properties of the gels was studied. As shown in Fig. 5(a), the gels with total monomer concentration C_m = 1.5 M, 0.5% chemical crosslinking density, and different fractions of acrylamide f = 5%, 30% and 100% were swelled by deionized water, 2.5 M NaCl solution with monovalent ions, 2.5 M CaCl$_2$ and 1.7 M BaCl$_2$ solutions with divalent ions, respectively. Please note that 1.7 M is already close to the solubility in water for BaCl$_2$ at room temperature. The as-prepared gel was synthesized in a Petri dish, and then the salt solution was added on top of the gel. The gel volume was measured every day until its volume did not change anymore, indicating that the gel has reached the swelling equilibrium. The volume fraction Φ of the gel is defined as:

$$\Phi = \frac{V_d}{V} = \frac{V_d}{V_0} \times \frac{V_0}{V} = \Phi_0 \times \frac{V_0}{V} \quad (2)$$

where V_d is the volume of the gel in the dried state, V is the

volume of the gel at swelling equilibrium, and V_0 is the volume of the gel in the as-prepared state. For the same gel sample, the volume fraction of the gel in the as-prepared state is $\Phi_0 = V_d/V_0$, so that the swelling ratio can be obtained from eqn (2) and expressed as $\Phi/\Phi_0 = V_0/V$.

As shown in Fig. 5(a), when swelled by water, the gel with f = 5% shrinks so that the final volume fraction increases to Φ/Φ_0 = 1.38. Because the ionic bonds would be strengthened and the ionic clusters would be more compact when swelled by water to remove the small ions, the gels would shrink. For gels with f = 30%, Φ/Φ_0 = 1.06 when swelled by water at swelling equilibrium, since the number of ionic bonds is less so that they would shrink less compared to that of the gels with f = 5%. While for pure polyacrylamide gels without ionic bonds (f = 100%), the gel swells to Φ/Φ_0 = 0.36 when swelled by water because the hydrogen bonds between water and acrylamide make the gel strands fully swollen in water. However, when these gels are swelled by monovalent or divalent salt solutions, all the gels swell at swelling equilibrium with $\Phi/\Phi_0 < 1$ (Fig. 5(a)) due to the screening of the electrostatic interactions for these ionic bonds. We did not observe the coordination complexation and bridging effect between the divalent ions and charged polyampholyte gels.[44,45] In fact, the divalent BaCl$_2$ solution can make the gels swell to the largest volume (smallest Φ/Φ_0). The swelling behaviors for different monomer concentrations at the fixed f = 5% were also investigated. As shown in Fig. 5(b), after swelling by water at swelling equilibrium, the gels with the smallest C_m = 1.0 M swell slightly with Φ/Φ_0 = 0.84 because the number of ionic bonds is not enough to make the gel shrink much, so that the osmotic pressure and Donnan equilibrium would dominate and make the gel swell slightly. While for gels with the largest C_m = 2.0 M, the swelling ratio is Φ/Φ_0 = 0.95, indicating that the gel volume changes slightly. Because the gels with higher C_m will have more topological entanglements, which act as permanent effective cross-linkers to suppress the large extent of shrinkage. As a result, only for the gels with intermediate monomer concentration C_m = 1.5 M,
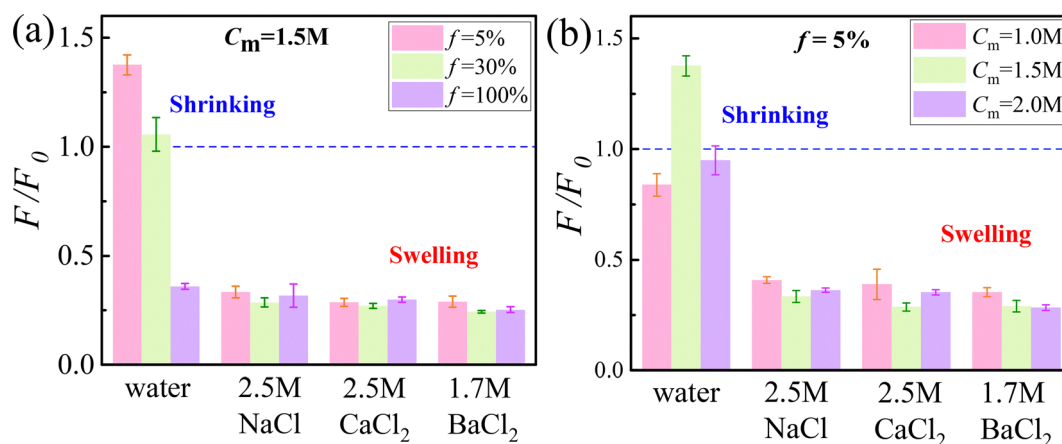

Fig. 5 Swelling ratio Φ/Φ_0 for (a) gels with C_m = 1.5 M and with different f, and (b) gels with f = 5% and with different C_m at swelling equilibrium. Gels are swelled by deionized water, 2.5 M NaCl, 2.5 M CaCl$_2$ and 1.7 M BaCl$_2$ solutions. Error bars reflect the standard deviation from three measurements of three replicate gel samples.
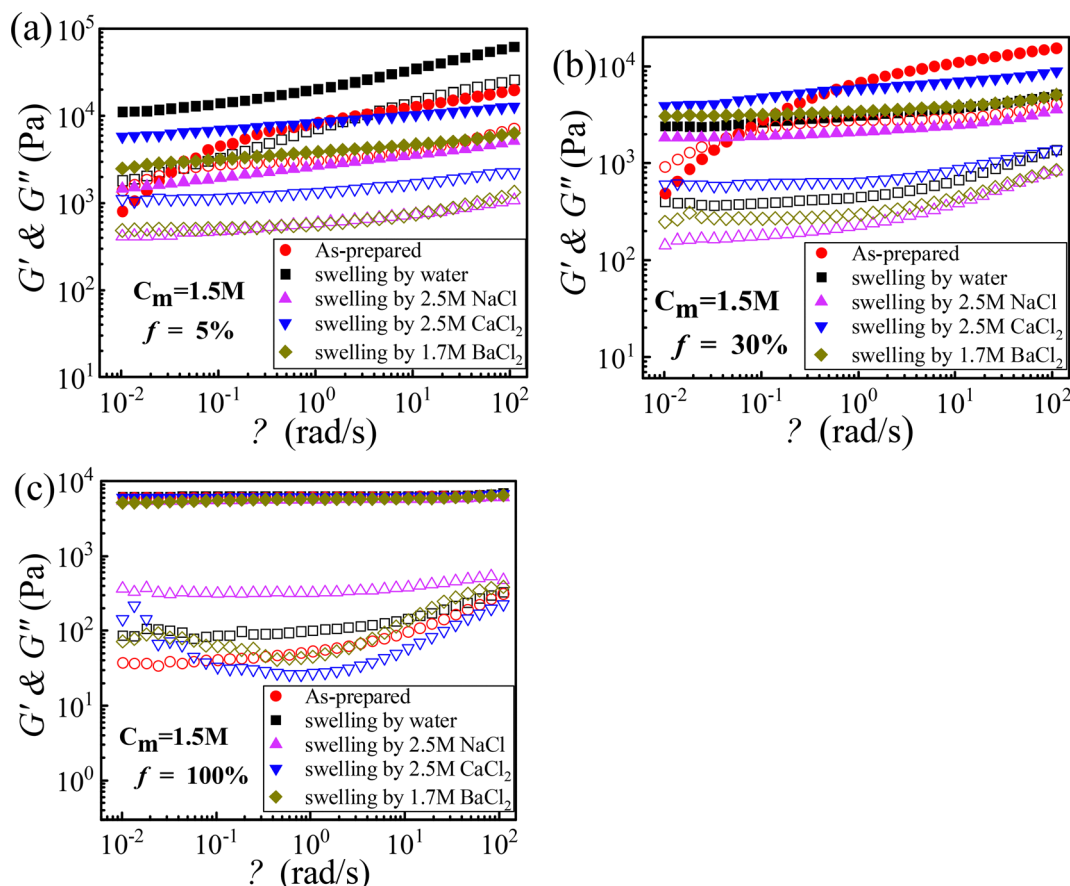
Fig. 6 Dynamic frequency sweeps for gels with fixed C_m = 1.5 M and different f, (a) f = 5%, (b) f = 30% and (c) f = 100%. Each sample was measured in different swelling states: as-prepared state, swelled by deionized water, swelled by 2.5 M NaCl, swelled by 2.5 M CaCl$_2$ and swelled by 1.7 M BaCl$_2$ solutions. The shear strain is fixed at γ = 1%. Closed (open) symbols represent the storage (loss) modulus.

they would shrink the most when swelled by water. While when the gels are swelled by salt solutions, the gels with different C_m all swell with $\Phi/\Phi_0 < 1$ at swelling equilibrium and exhibit a similar trend to that of the gels with different f due to the electrostatic screening.

Dynamic frequency sweeps were also conducted for the above swelling gels after they reached swelling equilibrium. For gels with f = 5% and 30% when the ionic bonds dominate, the crossover point ω_c of G' and G'' appears only for the as-prepared gels with intermediate ionic bond strength (Fig. 6(a) and (b)). As previously mentioned, such a crossover point ω_c may be due to the collective association–dissociation of the ionic clusters and the full relaxation of the topological entanglements. However, when the gels were swelled by deionized water to lower the ionic strength within the gels, the ionic bond strength would increase to form "permanent" bonds so that the association–dissociation dynamical behavior of these ionic bonds cannot be observed on the experimental time scale. On the other hand, when the gels were swelled by salt solutions to screen the electrostatic interactions of these ionic bonds, the crossover point ω_c would also be absent. In short, only with the intermediate ionic bond strength, the association–dissociation dynamical behavior of these ionic bonds with a crossover point ω_c can be observed. While the

ionic bond strength is too strong or too weak, the crossover point ω_c would disappear.

For gels with f = 5%, G' is the highest when the gels were swelled by water so that the ionic bond strength of the gels is the highest. When they are swelled by salt solutions, G' values all become smaller compared with those of the as-prepared gels (Fig. 6(a)). Please note that for both f = 5% and 30%, G' of the gels swelled by 2.5 M CaCl$_2$ solutions is more than 2.8 times higher than G' of the same gels swelled by 2.5 M NaCl solutions. Finally, for gels with f = 100%, it is pure polyacrylamide gels without ionic bonds, G' values do not change much after swelling by water and salt solutions (Fig. 6(c)). After swelling, the decrease of the volume fraction would make G' decrease, while the stiffening of the gel strands in the highly swollen gels would make G' increase.[46] Therefore, the two competing factors compensate for each other to make G' changes slightly after swelling (Fig. S6).

We also studied the yielding behaviors for the above gels at different swelling states. For gels with f = 5% swelled by water, the yielding point is γ_c = 8.3%, which is 46 times smaller than the same gel in the as-prepared state (γ_c = 384%) (Fig. 7(a)). For the as-prepared gels with intermediate ionic bond strength, the reversible association–dissociation dynamical process of these ionic bonds would provide excellent self-healing properties for
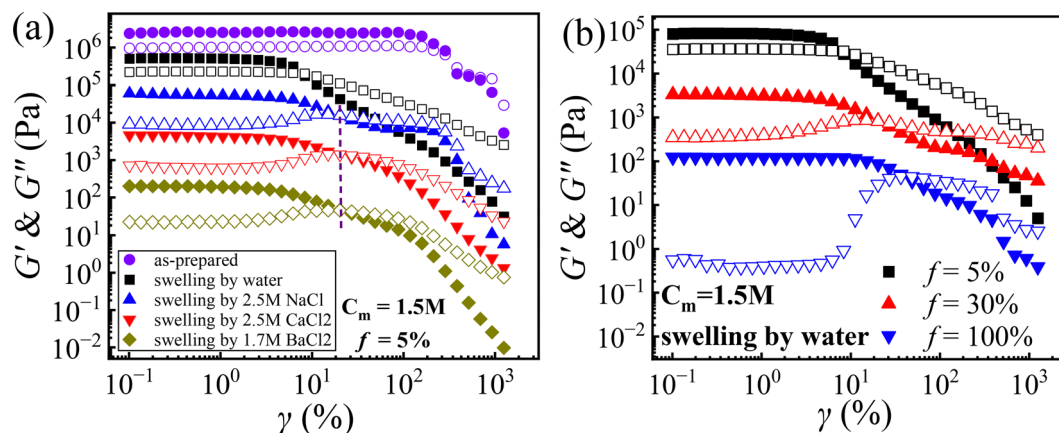
Fig. 7 (a) Shear strain sweeps at fixed frequency ω = 1 rad s^{-1} for gels at C_m = 1.5 M and f = 5% in different swelling states: as-prepared state, swelled by water, swelled by 2.5 M NaCl, swelled by 2.5 M CaCl$_2$ and swelled by 1.7 M BaCl$_2$ solutions. Closed (open) symbols represent storage (loss) moduli. (b) Shear strain sweeps at fixed frequency ω = 1 rad s^{-1} for gels swelled by water at C_m = 1.5 M and different f. For a clear vision, the data in (a) are shifted by 300×, 25×, 20×, 2/, 20/ from top to bottom, and the data in (b) are shifted by 4×, 52/, for f = 5%, 100%, respectively.

the gels during the deformation, thus they would yield at very large shear strain. However, when the gels are swelled by water to lower the ionic strength within the gels, the ionic bond strength would increase to form "permanent" bonds so that the self-healing properties arising from the association–dissociation of reversible ionic bonds would disappear, thus the gels swelled by water would be brittle and yield at very low shear strain. For gels swelled by high salt solutions, they all have γ_c = 20.2% (Fig. 7(a)). Now the ionic bonds would be screened at such high salt concentrations, so that their yielding behaviors are mainly dominated by the breakage of chemical bonds. In short, only for gels with intermediate ionic bond strength, they would exhibit excellent self-healing properties with a large yielding point γ_c.

Moreover, the gels with different fractions of acrylamide f after swelled by water were also investigated. As f increases from 5% to 100%, the yielding point increases slightly from 8.3% to 48.8% (Fig. 7(b)). Although the self-healing properties disappear for gels swelled by water, hydrogen bonds would also provide extra support to protect the gels during deformation when hydrogen bonds dominate in the gels with larger f. Besides, for the pure polyacrylamide gels (f = 100%) with 0.5% chemical crosslinking density, the yielding point for gels swelled by water (γ_c = 48.8%) (Fig. 7(b)) is more than four times smaller than that of the same gels in the as-prepared state (γ_c = 213%) (Fig. 3(b)). This is probably because after swelling by water, the number of hydrogen bonds between amide groups and water molecules increases so that the number of hydrogen bonds between amide and amide groups within the polyacrylamide gels decreases, leading to less hydrogen bonds between polymer strands within the gel network to support and protect the gels during the deformation.

Conclusions

In summary, we have studied the interplay between the hierarchical structures and the viscoelastic properties of the polyampholyte gels by introducing the acrylamide neutral blocks. During the dynamic frequency sweeps in the linear viscoelastic region, a crossover point ω_c of G' & G'' would occur due to the collective dynamical behavior of association–dissociation of the ionic clusters and the full relaxation of the topological entanglements. As the fraction of acrylamide neutral blocks f increases, the interlude of the neutral acrylamide blocks would make the size and density of the ionic clusters smaller, leading to a higher ω_c and a shorter relaxation time. As f further increases, both G' & G'' would exhibit less frequency dependence and the gels gradually transfer from physical gels to chemical gels. Moreover, the VSANS technique is used to explore the microstructures of the gels, and it was found that the interlude of hydrophilic acrylamide neutral blocks will act as defects to suppress the phase separation and make the microphase separated domains become smaller. During the yielding measurements in the nonlinear viscoelastic region, the reversible dissociation–association dynamical process of the ionic bonds can support and protect the gel network from yielding, offering the gels excellent self-healing properties. As f increases, the interlude of acrylamide neutral blocks would act as defects to disrupt the formation of the ionic bonds, thus making the yielding point γ_c decrease. And the hydrogen bonds between acrylamide groups would also protect the gels during deformation, so that the yielding points exhibit non-monotonic f dependence. Finally, the impact of different swelling methods on the viscoelastic properties of the gels was also studied. Only for gels with intermediate ionic bond strength, would they exhibit excellent self-healing properties with large yielding points γ_c, and the crossover point ω_c would show up in the dynamical frequency sweeps due to the association–dissociation collective dynamical behavior of the ionic bonds. While when the ionic bond strength is too strong or too weak, the self-healing properties would disappear and the crossover point ω_c would also be absent. This work provides physical guidance to precisely tune the self-healing behaviors and viscoelastic properties of polyampholyte gels applied in various fields such as biomaterials and bioengineering.

Author contributions

Conflicts of interest

There are no conflicts to declare.

Data availability

All data discussed in the paper are available in the main text and the SI. Supplementary information: NMR spectra of gels, VSANS data for gels and rheological measurement results for gels. See DOI: **https://doi.org/10.1039/d5sm00407a**

Acknowledgements

References

1 J. P. Gong, Y. Katsuyama, T. Kurokawa and Y. Osada, *Adv. Mater.*, 2003, **15**, 1155–1158.

2 M. Du, H. A. Houck, Q. Yin, Y. Xu, Y. Huang, Y. Lan, L. Yang, F. E. Du Prez and G. Chang, *Nat. Commun.*, 2022, **13**, 3231.

3 A. B. Ihsan, T. L. Sun, T. Kurokawa, S. N. Karobi, T. Nakajima, T. Nonoyama, C. K. Roy, F. Luo and J. P. Gong, *Macromolecules*, 2016, **49**, 4245–4252.

4 Y. Huang, L. Xiao, J. Zhou, T. Liu, Y. Yan, S. Long and X. Li, *Adv. Funct. Mater.*, 2021, **31**, 2103917.

5 Y. Jin, S. Lu, X. Chen, Q. Fang, X. Guan, L. Qin, C. Chen and C. Zhao, *Macromolecules*, 2024, **57**, 2746–2755.

6 J. P. Gong, *Soft Matter*, 2010, **6**, 2583–2590.

7 G. Toleutay, E. Su and G. Yelemessova, *Polymers*, 2023, **15**, 3131.

8 X.-H. Wang, F. Song, D. Qian, Y.-D. He, W.-C. Nie, X.-L. Wang and Y.-Z. Wang, *Chem. Eng. J.*, 2018, **349**, 588–594.

9 M. Zhang, Y. Yang, M. Li, Q. Shang, R. Xie, J. Yu, K. Shen, Y. Zhang and Y. Cheng, *Adv. Mater.*, 2023, **35**, e2301551.

10 H. Fan, J. Wang and Z. Jin, *Macromolecules*, 2018, **51**, 1696–1705.

11 Y. Ye, Z. Wan, P. D. S. H. Gunawardane, Q. Hua, S. Wang, J. Zhu, M. Chiao, S. Renneckar, O. J. Rojas and F. Jiang, *Adv. Funct. Mater.*, 2024, **34**, 2315184.

12 D. Mu and J. Xing, *Colloids Surf., A*, 2023, **671**, 131656.

13 T. L. Sun, T. Kurokawa, S. Kuroda, A. B. Ihsan, T. Akasaki, K. Sato, M. A. Haque, T. Nakajima and J. P. Gong, *Nat. Mater.*, 2013, **12**, 932–937.

14 S. L. Haag and M. T. Bernards, *Gels*, 2017, **3**, 41.

15 C. K. Roy, H. L. Guo, T. L. Sun, A. B. Ihsan, T. Kurokawa, M. Takahata, T. Nonoyama, T. Nakajima and J. P. Gong, *Adv. Mater.*, 2015, **27**, 7344–7348.

16 P. Rao, T. L. Sun, L. Chen, R. Takahashi, G. Shinohara, H. Guo, D. R. King, T. Kurokawa and J. P. Gong, *Adv. Mater.*, 2018, **30**, 1801884.

17 X. Li, K. Cui, Y. Zheng, Y. N. Ye, C. Yu, W. Yang, T. Nakajima and J. P. Gong, *Sci. Adv.*, 2023, **9**, eadj6856.

18 X. Li, K. Cui, T. Kurokawa, Y. N. Ye, T. L. Sun, C. Yu, C. Creton and J. P. Gong, *Sci. Adv.*, 2021, **7**, eabe8210.

19 K. Cui, Y. N. Ye, T. L. Sun, C. Yu, X. Li, T. Kurokawa and J. P. Gong, *Macromolecules*, 2020, **53**, 5116–5126.

20 X. Li and J. P. Gong, *Proc. Natl. Acad. Sci. U. S. A.*, 2022, **119**, e2200678119.

21 K. Cui and J. P. Gong, *J. Rheol.*, 2022, **66**, 1093–1111.

22 X. Li, K. Cui, T. L. Sun, L. Meng, C. Yu, L. Li, C. Creton, T. Kurokawa and J. P. Gong, *Proc. Natl. Acad. Sci. U. S. A.*, 2020, **117**, 7606–7612.

23 X. Y. Li, F. Luo, T. L. Sun, K. P. Cui, R. Watanabe, T. Nakajima and J. P. Gong, *Macromolecules*, 2023, **56**, 535–544.

24 K. Cui, C. Yu, Y. N. Ye, X. Li and J. P. Gong, *Proc. Natl. Acad. Sci. U. S. A.*, 2022, **119**, e2207422119.

25 C. Yu, H. Guo, K. Cui, Y. N. Ye, T. Kurokawa and J. P. Gong, *Proc. Natl. Acad. Sci. U. S. A.*, 2020, **117**, 18962–18968.

26 J. P. Baker, D. R. Stephens, H. W. Blanch and J. M. Prausnitz, *Macromolecules*, 1992, **25**, 1955.

27 D. G. Peiffer and R. D. Lundberg, *Polymer*, 1985, **26**, 1058.

28 T. Zuo, Z. Han, C. Ma, S. Xiao, X. Lin, Y. Li, F. Wang, Y. He, Z. He, J. Zhang, G. Wang and H. Cheng, *J. Appl. Crystallogr.*, 2024, **57**, 380–391.

29 Z. Han, C. Ma, H. Zhu, T. Cui, T. Zuo and H. Cheng, *J. Appl. Crystallogr.*, 2024, **57**, 1772–1779.

30 D. Jia, J. V. Hollingsworth, Z. Zhou, H. Cheng and C. C. Han, *Soft Matter*, 2015, **11**, 8818–8826.

31 Z. Zhou, D. Jia, J. V. Hollingsworth, H. Cheng and C. C. Han, *J. Chem. Phys.*, 2015, **143**, 234901.

32 D. Jia, H. Cheng and C. C. Han, *Langmuir*, 2018, **34**, 3021–3029.

33 S. Zhang, D. Ren, Q. Zhao, M. Peng, X. Wang, Z. Zhang, W. Liu and F. Huang, *Nat. Commun.*, 2025, **16**, 2371.

34 L. Tavares and C. P. Z. Noreña, *J. Food Meas. Charact.*, 2022, **16**, 295–306.

35 Y. H. Zhao, Y. S. Jie, Y. C. Xue, Z. W. Shi, Y. Ch Dong, M. Muthukumar and D. Jia, *Nat. Commun.*, 2025, **16**, 3247.

36 D. Jia and M. Muthukumar, *Macromolecules*, 2019, **53**, 90–101.

37 J. D. Ferry, *Viscoelastic properties of polymers*, John Wiley & Sons, 1970.

38 Z. Zhang, Q. Chen and R. H. Colby, *Soft Matter*, 2018, **14**, 2961–2977.

39 Y. Liu, B. Momani, H. H. Winter and S. L. Perry, *Soft Matter*, 2017, **13**, 7332–7340.

40 T. Vermonden, N. A. M. Besseling, M. J. van Steenbergen and W. E. Hennink, *Langmuir*, 2006, **22**, 10180–10184.

41 D. A. Dixon, K. D. Dobbs and J. J. Valentini, *J. Phys. Chem.*, 1994, **98**, 13435–13439.

42 E. Spruijt, S. A. van den Berg, M. A. Cohen Stuart and J. van der Gucht, *ACS Nano*, 2012, **6**, 5297–5303.

43 M. Rubinstein and R. H. Colby, *Polymer Physics*, Oxford University Press, New York, 2003.

44 S. Samanta, S. Kim, T. Saito and A. P. Sokolov, *J. Phys. Chem. B*, 2021, **125**, 9389–9401.

45 X. Zhao, X. Chen, H. Yuk, S. Lin, X. Liu and G. Parada, *Chem. Rev.*, 2021, **121**, 4309–4372.

46 S. Morozova and M. Muthukumar, *Macromolecules*, 2017, **50**, 2456–2466.